OPTIMIZATION OF AGRO-WASTE: HARNESSING OIL PALM PRESSED FIBRE FOR ADVANCED BIOPLASTIC SYNTHESIS WITH EXCEPTIONAL MECHANICAL PROPERTIES

Supported by tetfund
TERTIARY EDUCATION TRUST FUND

Ayorinde. O. Nejo[1]* and Taiwo. S. Aiyelero[2]
[1] Chemistry Department, Faculty of Science University of Lagos, Nigeria
[2] Department of Chemical Science, College of Basic Science, Lagos State University of Science and Technology, Ikorodu Lagos
*Corresponding Author; funaina2014@gmail.com

Received: January 10, 2024 Accepted: March 28, 2024

Abstract: The degradability of plastic has been a serious challenge to man and its environment prompting the need for an intervention in the form of biodegradable plastics. Some of the challenges include; environmental pollution, microplastic contamination, toxic chemical leaching and greenhouse gas emission. This study focuses on the extraction of cellulose from oil palm pressed fiber (OPF) and its subsequent conversion into cellulose nanocrystals (CNC) and cellulose acetate for bioplastic synthesis which will solve some of the listed challenges. The uniqueness of this cellulose-based bioplastic is the fact that toxic chemical leaching would not be a problem as it does not utilize harmful chemicals such as phthalates and BPA (Bisphenol A). The materials and methods include the isolation of cellulose from OPF through chemical treatments, CNC production through maleic acid hydrolysis, cellulose acetate preparation, and bioplastic synthesis. Experimental analyses cover percentage yield determination, hemicellulose and lignin determination, proximate analysis, and functional property evaluations. The results highlight the successful extraction of cellulose, with hemicellulose being the major component, and the subsequent production of CNC and cellulose acetate. The bioplastic synthesized demonstrated significant degradation of an average mass of 86.26% over a 28 days period, indicating its environmental friendliness. Mechanical properties such as hardness shows that the higher the content of glycerol, the less the hardness; tensile strength increased as the amount of glycerol was increased showing a remarkable strength of 6.08 MPa as the minimum (without glycerol) exceeding the minimum value of 1.343 MPa according to the Biodegradable plastic standard SNI 7818:2014; elongation characteristics showed the interaction between glycerol and the cellulose acetate increased the stretching ability of the bioplastic but further addition of the glycerol only caused a slightly significant elongation. XRD and SEM analyses revealed changes in crystallinity and morphology during the bioplastic synthesis process. FT-IR spectra confirmed the chemical modifications, and the degree of substitution for cellulose acetate was determined. The study provides valuable insights into the sustainable utilization of OPF for eco-friendly bioplastic production with desirable mechanical and degradation properties.

Keywords: Cellulose, Cellulose Acetate, Bioplastics, Nanoparticles

Introduction

As the primary structural element of both lower and higher plants' cell walls, cellulose is the most prevalent biopolymer (Feng and You, 2015). This polymer comprises of glucose subunits. The cell walls of both bacteria and plants contain large amounts of it. In stalks, stems, and other woody plant components, we find substantial cellulose content. Algae and fungi also include cellulose in their cell walls, in contrast to bacteria, which only seldom possess it. Bacteria that produce acetic acid can also produce cellulose, much like higher plants do. Bacterial cellulose is extremely pure, in contrast to plant cellulose, which is usually mixed with lignin, hemicelluloses, and pectin (Yang *et al*., 2016).

Cellulose exhibits a wide range of exceptional physicochemical and mechanical characteristics, including high crystallinity, a high degree of polymerization, high water-absorbing and water-holding capabilities, high tensile strength, high elasticity, outstanding biocompatibility, and biodegradability (De-france *et al.*, 2017).

Due to their biocompatibility, biodegradability, and low cytotoxicity, cellulosic materials in particular hold out a lot of potential as affordable, futuristic materials for biomedical applications. Furthermore, cellulosic materials are simple to modify to produce valuable products due to their chemical activity. Water spreads and absorbs more readily by capillary action between the cellulose fibers thanks to the rough and porous surface characteristics of paper and cotton textiles. Capillary-driven liquid transportation is used, for instance, in paper-based microfluidic systems (Li *et al.*, 2013). Due to its abundance, biodegradability, and special physical, chemical, and mechanical properties, cellulose offers unparalleled advantages as a super-hydrophobic material substrate when compared to commonly use non-renewable materials, despite its inherent hydrophilicity (Song and Rojas, 2013). Traditional methods of disease prevention and healthcare are incredibly dependent on cellulosic materials. The exploration of several new application areas continues, including tissue engineering (Ninan *et al.*, 2013), wound healing (Solway *et al.*, 2011), and medication delivery (Gunduz *et al.*, 2013). Research on model herbaceous plants and fiber crops produced the majority of the most recent results about the molecular process of cellulose manufacture in higher plants, and these findings have recently been reviewed (Somerville, 2006).

Depending on its source, naturally occurring bulk cellulose has a mixture of highly ordered, crystalline areas and some disordered (amorphous) parts in variable quantities. The highly crystalline sections of these microfibrils may be

removed, resulting in the development of cellulose nanocrystals (CNCs), when they are treated to the right mix of mechanical, chemical, and enzyme treatments (Domingues *et al.*, 2014). A very flawless crystalline structure makes up the rigid rod-like CNCs, which are made of cellulose chain segments. The most popular nomenclature for these nanocrystals is CNCs (Habibi *et al.*, 2010), however they can also be referred to as whiskers, nanoparticles, nanofibers, microcrystallites, and so on. These nanocrystals display high specific strength, modulus, large surface area, and particular liquid crystalline characteristics in contrast to bulk cellulose, which has higher amorphous fractions.

According to Lam *et al.* (2012), CNCs have a lot of advantageous physical and chemical characteristics, including a high surface area (250 m^2/g), a high tensile strength (7500 MPa), a high stiffness (Young's modulus up to 140 GPa), and a lot of surface hydroxyl groups. These surface hydroxyl groups provide an easy platform for chemical modification; for example, they might be changed into carboxylic acid, acetate, amine, aldehyde, or thiol groups.

The contemporary world was built with the help of plastics and other common polymers made from fossil feedstocks. Due of its lengthy durability in terrestrial and aquatic settings, plastic has degraded ecosystems, imperiled marine life, and caused concerns to human health (Jiang and Ngai, 2022). Several studies have been conducted using organic and biodegradable polymers to create edible packaging films. Biodegradable polymers have a wider range of waste management choices than traditional plastics. Recently, the production of biodegradable materials from renewable natural resources, such as plants, has received increased attention. This is especially true in European countries, where the use of renewable resources has been revitalized. If correctly handled, this would reduce their environmental effect when disposed of, and it is both technically and financially possible (Rohmawati *et al.*, 2018). In order to create affordable biodegradable and edible films, the polymer matrix and reinforcement should be obtained from abundant and renewable resources. For producing edible films made of starch that have a stronger water vapor barrier and mechanical characteristics, CNCs are an intriguing reinforcement (Rhim *et al.*, 2013). Applications for agglomerated CNCs are limited since they are challenging to disperse physically. To enhance re-dispersion, CNCs can be made more hydrophobic. The hydrophobic alteration of CNC surfaces has drawn a lot of attention since these materials are more suited for usage with water-insoluble polymers like polyolefins. The creation of cellulose acetate by the acetylation of cellulose enhances the performance of bioplastics. Agro-industrial residue is gaining popularity as a competitive substitute for raw cellulosic materials because of its accessibility, low lignin content, quick growth cycles, fiscal responsibility, and environmental friendliness. Approximately 800 million dry tons of agricultural residues are generated each year throughout the world, and these residues are discarded in huge quantities in open areas or municipal bins, which results in environmental issues (Kassab *et al.*, 2020).

Materials and Methods

Materials

Oil palm pressed fibre was obtained from a farm at Lagos state university of science and technology, Ikorodu Lagos, Nigeria, sodium hydroxide (Sigma-Aldrich ≥ 98% pellets), sodium sulphite anhydrous (Sigma-Aldrich ≥ 98% pellets), nitric acid (Emsure 65%), hydrochloric acid (Emsure 37%), ethanol (Emsure 37%), Sodium hypochlorite 3.5% (w/v), sulphuric acid (Emsure 95 - 97%), freshly prepared distilled water and maleic acid (Sigma-Aldrich ≥ 99% pellets).

Preparation of Samples

1 kg of the oil palm pressed fibres were sorted to get only fibre, washed thoroughly before air- drying for a few days and then ground into fine powder.

Cellulose Isolation (oil palm pressed fibre)

500 g of the powdered fibers were macerated with 10 % nitric acid and 0.8 % sodium sulphite, delignified between 85 ºC and 95 ºC for 3 hour, rinsed and filtered many times. Alkaline treatment was done on the delignified sample using 4% sodium hydroxide and 0.8% sodium sulphite for 2 hours. This was followed by bleaching with sodium hypochlorite at 60 °C in a hot water bath for 15 minutes until whiteness was obtained to give white chemically purified extracted cellulose. The resulting cellulose was washed thoroughly with distilled water. Finally, the residue was air-dried and the percentage yield of the cellulose was determined.

CNC Production

Maleic acid hydrolysis of the extracted cellulose was carried out using a liquid to pulp weight ratio of 100:1 in a maleic acid solution (Seta *et al.*, 2020). Reaction was continuously stirred for 3 hours, after which it was quenched with de-ionized water. The sample was then separated by filtration through a cheese cloth.

Preparation of Cellulose Acetate

Cellulose was acetylated using the technique described by Lawal *et al.* in 2005. Using this approach, 10g of cellulose was dissolved in 50ml of distilled water and swirled for 20 min using a magnetic stirrer. NaOH was added to control the pH slightly above neutral over an hour while adding 60ml of acetic anhydride and keeping the temperature at 60 ºC. It underwent filtration, constant washing and weight-stabilizing air drying at 30°C.

Bioplastic Synthesis

The method adopted was modified from Rohmawati *et al.*, 2018. A 15 ml solution of 0.665 M acetic acid was added to 0.80 grams of dry cellulose acetate. It was mixed for 15 minutes while 0.4 g of chitosan and glycerol were added. The slurry was cast and oven dried at 60 ºC for 1 hour. The experiment was repeated by varying the glycerol volume (0 ml, 1 ml and 2 ml).

Experimental Analysis

Percentage Yield

The percentage yield of the cellulose was estimated by comparing the dried mass of the isolated cellulose with the mass of the starting material:

Percentage Yield (%) = $\frac{\text{Mass of cellulose} \times 100}{\text{Mass of sample}}$

Determination Of Hemicellulose

150 mL of sodium hydroxide (NaOH) solution (0.5 mol/L) was added to 2 g of Oil palm pressed fiber with extractives free. The temperature of 80 °C was controlled by using a hot plate for 3.5 hours. After that, the sample was washed with deionized water until it was free from Na^+. The sample was oven dried between 105 – 110 °C.

Determination of Lignin

30 mL of 98 % sulphuric acid was added to 2 g of Oil palm pressed fiber with extractives free. The sample was left at ambient temperature for 24 hours before being boiled at a temperature of 100 °C controlled by using a hot plate for 1 hour. This was followed by filtration and washing until sulfate ion was undetectable. Detection of sulfate ion was done via titration process with 10 % of barium chloride solution. The sample was oven dried between 105 – 110 °C. The final weight of residue is recorded as lignin content.

Proximate Analysis

Determination of Moisture Content

2 g each of cellulose was placed in pre-weighed crucibles and heated in an oven at 105 °C for 3 hours. The heated samples were weighed on an analytical balance. The following calculation was then performed to know the moisture content of each sample;

$M_n = \frac{Ww - Wd}{Ww} \times 100$

Where;

M_n= moisture content of the material.
W_w = Mass of the sample (g).
W_d = Mass of the sample after drying (g).

Determination of Total Ash

1 g of cellulose was added to each labeled crucible and the weight of the crucible plus sample was determined as (W_2) and transferred into the muffle furnace to ash at 550 °C for 4 h. The crucibles were allowed to cool in a desiccator and reweighed as (W_3). Percentage ash was calculated and the ash was used for mineral analysis.

Ash Content (%)= $\frac{\text{Mass of Ash} \times 100}{\text{Mass of sample}}$

Ash Content (%) = $\frac{W3 - W1}{W2 - W1} \times 100$

Where W_1 = Mass of empty crucible,
W_2 = Mass of the crucible and sample,
W_3 = Mass of the crucible and ash sample

Determination of Crude Fat

The crude fat was determined by the Soxhlet extraction system using the method of (Lawal *et al.*, 2005). A dried filter paper was weighed as (W_1). 2.5 g of the cellulose was added in the filter paper, weighed as (W_2). This was placed in the Soxhlet extractor refluxed for 8 hours. The filter paper and defatted samples were dried in the oven at 50 °C for about 30 minutes and weighed as (W_3).

% Crude fat = $\frac{W3 - W2}{W2 - W1}$ x 100

Where W_1 = Mass of the filter paper
W_2 = Mass of the filter paper and the sample
W_3 = Mass of the defatted sample and the filter paper

Swelling Power

0.5 g of cellulose samples were transferred into a dried test tube and weighed (w_1). 10 ml of distilled water was added to the test tube and the mixture was mixed thoroughly. The slurries were heated at temperatures of 80 °C for 30 minutes in a water bath and centrifuged at 5000 rev/min. the final weight was taken as W_2.

Swelling of cellulose = $\frac{W2 - W1}{W1} \times 100$

Determination of Functional Properties

The obtained Cellulose was analyzed for bulk density, packed density, hydrated density, water retention capacity, and oil retention capacity.

Bulk Density

10g of the sample was filled into a pre-weighed syringe. The volume and mass were recorded, and the bulk density was expressed as mass per volume.

The bulk density was calculated using the following equation:

Bulk density (g/ml) = $\frac{\text{Mass of the sample (g)}}{\text{Volume of the sample (ml)}}$

Packed Density

Known mass of the sample were compressed into a 20ml syringe until additional pressure would not further decrease the volume. The packed density was calculated as the mass of the sample per least volume of the sample.

The packed density shall be calculated using the following equation:

Packed density (g/ml) = $\frac{\text{Mass of the sample}}{\text{Least volume of the}}$

Hydrated Density

A 10 ml syringe was filled with a known amount of distilled deionized water, and a known mass of the sample was added. The difference between the volume of the water before and after adding the sample was recorded as volume of water displaced.

Hydrated density (g/ml) = $\frac{\text{Mass of sample (g)}}{\text{Displaced volume of sample (ml)}}$

Water Retention Capacity (WRC) and Oil Retention Capacity (ORC)

5 g of sample was mixed with 15 ml of distilled water in a 50 ml centrifuge tube. The slurry was centrifuged at 2000 rev/min for 15 minutes. The precipitate was weighed and expressed as gram of water per gram of the sample. For the ORC, soya oil was used instead of water.

The WRC and ORC were calculated using the following equation:

Water retention capacity= $\frac{\text{Mass of supernatant (g water / g dried sample)}}{\text{Mass of precipitate}}$

Oil retention capacity= Mass of supernatant (g oil / g dried sample)
Mass of precipitate

Determination of Degree of Substitution of Cellulose Acetate

The degree of substitution was calculated using Lawal *et al.* (2005). 5 g of acetylated cellulose was poured into a 250 ml flask with 50 ml of distilled water. After adding a few drops of phenolphthalein indicator, the suspension was titrated with 0.1 M sodium hydroxide until it reached a permanently pink end point. After adding 25 ml of 0.45 M sodium hydroxide solution, the flask was shaken ferociously for 30 minutes while being firmly closed with a rubber stopper. The mixture that had been saponified and then titrated with a standard solution of 0.2 M HCl until the phenolphthalein color vanished.

Percent acetyl in dry basis (A) = (Blank titre - Sample titre) ml ×Acid Molarity × 0.043 × 100
Sample weight in g (Dry basis)

Degree of Substitution (D.S) = 162 A
4300 – 42A

In which A = percent acetyl (dry basis).

Characterisation

X-Ray Diffraction Method (XRD): The cellulose and the functionalized products were subjected to XRD analysis, crystallinity and crystallite size estimated using the equations…

$$CrI = \frac{(I_{cr} - I_{am})}{I_{cr}} \times 100 \quad (3.9)$$

$$t(nm) = \frac{k \times \lambda}{\beta Cos\theta} \quad (3.10)$$

Where I_{cr} is the diffraction peak with highest intensity corresponding to the lattice plane and I_{am} is the diffraction intensity corresponding to the amorphous area; B_r = FWHM (full width at half maximum of the peak) in radian, t is crystallite size (nm), λ is wavelength (nm), *K* is a dimensionless shape factor 0.94, θ is Bragg angle in radian.

Fourier Transform Infrared Spectroscopy (FT-IR)

The various functional groups present in the extracted CNC and its derived acetate by FT-IR.

Scanning Electron Microscope (SEM) Analysis

Surface granule morphology of the extracted and modified cellulosic fibres were examined using scanning electron microscopic tool. A thin layer of sample granule was placed on aluminium specimen holder by doublesided tape. The specimen holder was loaded in a polaron SC 7610 sputter coater and coated with gold to a thickness of about 30 nm to prevent charging. The specimen holder was transferred to XL-20 series. Scanning electron microscope of cellulose and the derivatives were examined at an accelerating voltage of 15–20 kV

3.6.4 DEGRADATION ABILITY OF BIOPLASTIC

Bioplastic degradation tests were performed by burying all bioplastic samples for 28 days. The percentage loss of mass from bioplastics will be known through this analysis. We can determine percent loss of mass of the three bioplastic samples through the equation:

Mass Loss (%) = $\frac{Wi - Wf}{Wi}$ x 100%

Wi: bioplastic mass before degradation

Wf: bioplastic mass after degradation

Mechanical Properties of Bioplastic

1. Hardness Test

The Brinell method was used for the testing of the material, since its Polymeric in nature. In the Brinell hardness test, an optical method, the size of indentation left by the indenter is measured. In contrast to the likewise optical Vickers method which involves a pyramid-shaped indenter being pressed into a specimen (sample), the Brinell method uses a spherical indenter to hit the sample for the test. The larger the indent left in the surface of a work piece (sample) by the Brinell indenter with a defined ball diameter and a defined test force, the softer the tested material.

2. Tensile Strenght And Elongation

The Universal testing machine (UTM-D2) was used. Operation of the machine is by hydraulic transmission of load from the test specimen to a separately housed load indicator. Load is applied by a hydrostatically lubricated ram. Main cylinder pressure is transmitted to the cylinder of the pendulum dynamometer system housed in the control panel. The cylinder of the dynamometer is also of self-lubricating design. The load transmitted to the cylinder of the dynamometer is transferred through a lever system to a pendulum. Displacement of the pendulum actuates the rack and pinion mechanism which operates the load indicator pointer and the autographic recorder. The deflection of the pendulum represents the absolute load applied on the test specimen. Return movement of the pendulum is effectively damped to absorb energy in the event of sudden breakage of specimen. For the samples a uniform dimension was used viz:

i. thickness – 0.05 mm
ii. width – 10 mm
iii. length – 40 mm

Results and Discussion

Figure 4: (a) Untreated oil palm fibre (b) Acid Hydrolyzed oil palm fibre

(c) Alkaline Treated oil palm fibre

(d) Cellulose from oil palm fibre

(e) Hemicellulose from oil palm fibre

(f) Lignin oil palm fibre

Figures 4 provide a visual analysis of the oil palm pressed fiber (OPF) from its raw state through each stage of chemical treatment (a, b, c, d, e and f). The raw material was brown in colour before chemical processing. Following the acid hydrolysis stage, a color shift to golden yellow was seen, indicating that the raw sample's basic lignin and hemicellulose had been eliminated. The alkali treatment stage turned the color into deep gray, confirming the elimination of any remaining lignin and acidic hemicellulose. The cellulose sample after bleaching was entirely white. Hemicellulose had a deep brown coloring, while lignin showed a black coloration; this result is consistent with the research published by Kumar *et al* (2017). As can be seen in Table 1, the percentage yields of cellulose, lignin, and hemicellulose are 38.45 %, 15.78 %, and 45.77 %, respectively for OPF cellulose. Based on the obtained data, it was discovered that Hemicellulose made up a larger percentage of the cell wall.

Percentage Yield of Cellulose, Hemicellulose and Lignin

Table 1: Percentage yield of Cellulose, Hemicellulose and Lignin

SAMPLE	YIELD (%)
Cellulose	38.45
Lignin	15.78
Hemicellulose	45.77

Table 2: Functional properties of Cellulose and Cellulose Nano-crystals.

SAMPLE	(g/mL) Bulk density	(g/mL) Packed density	(g/mL) Hydrated density	(g/g) WRC	(g/g) ORC
IC	0.20	0.39	1.0	0.48	0.89
CNC	0.27	0.58	1.03	0.45	0.64

IC: Isolated cellulose; CNC; Cellulose Nanocrystal; WRC: water retention capacity; ORC: Oil retention capacity.

Table 2 displays the findings of the functional properties of the cellulose and cellulose nanocrystal. The difference in particle size causes the bulk density of the cellulose, and the amount of water that cellulose displaces is what causes the increased hydrated density. Because of the cellulose's strong binding formation, it can hold onto oil far better than water (Kristina *et al*., 2004). The hydrated density of the cellulose was greater than the packed density. The increase in crystallinity in the sample for the CNC caused an increase in bulkiness of the samples from (0.31 g/mL to 0.42 g/mL).

XRD Results

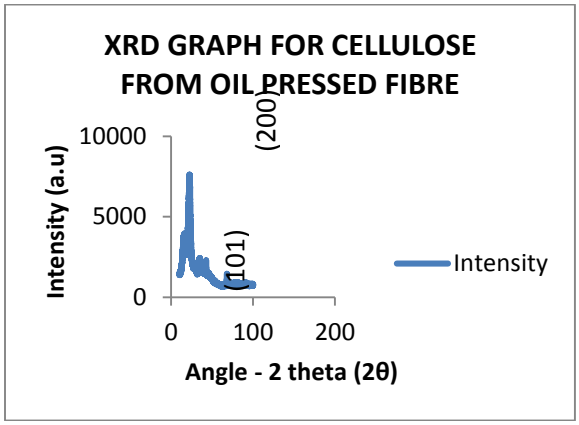

Figure 5: (a) Cellulose

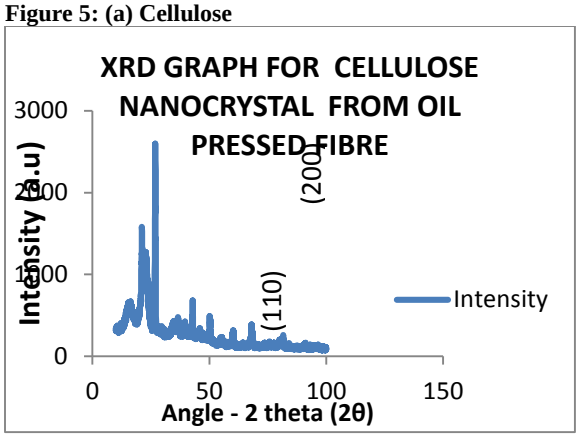

Figure 5: (b) Cellulose Nanocrystal

Fig.5(a) shows the XRD graph of the cellulose having about five distinct peaks showing the main crystalline regions and more amorphous regions for the cellulose, while the result of (b) have more notable peaks at points where the amorphous regions have disintegrated to give rise to more crystalline regions.

XRD of the synthesized bioplastic

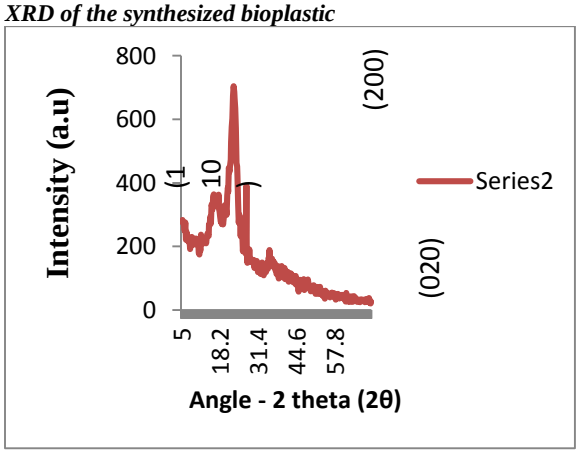

Figure 5: XRD graph showing intensity peaks and the corresponding angle of synthesized bioplastic from Oil Palm Pressed fibre (a)Without glycerol (0ml)

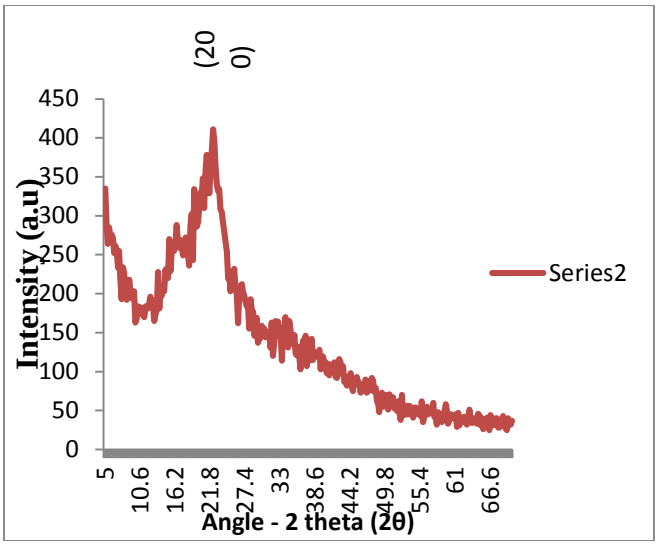

Figure 5: XRD graph showing intensity peaks and the corresponding angle of synthesized bioplastic from Oil Palm Pressed fibre (b) with glycerol (1ml)

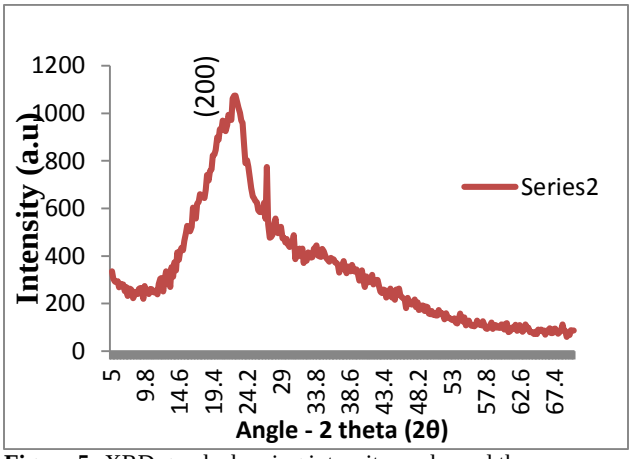

Figure 5: XRD graph showing intensity peaks and the

Corresponding angle of synthesized bioplastic from oil palm pressed fibre (c) with glycerol (2 ml)

Fig.5(a) shows the XRD graph of the synthesized bioplastic having about three distinct peaks showing the main crystalline regions from the OPF route, at this stage no glycerol was added while the result of (b) have lesser peaks (two pronounced peaks) and more amorphous regions which could be attributed to the glycerol been added. In (c) another two distinct peaks were observed. The lesser crystalline peaks are due to the addition of the glycerol.

SEM Micrograph

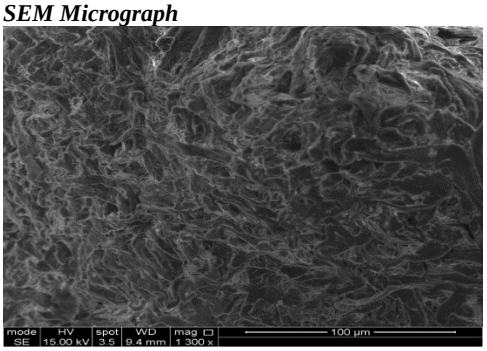

Figure 6: SEM micrograph showing the morphology (a) Cellulose (OPF)

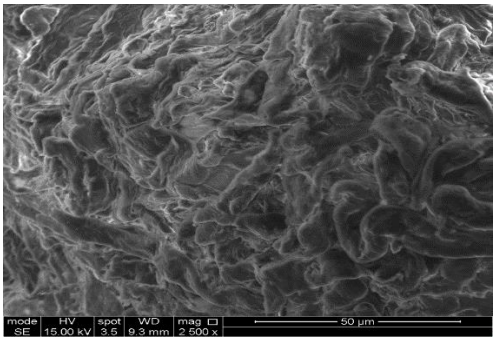

Figure 6: SEM micrograph showing the morphology (b) CNC (OPF)

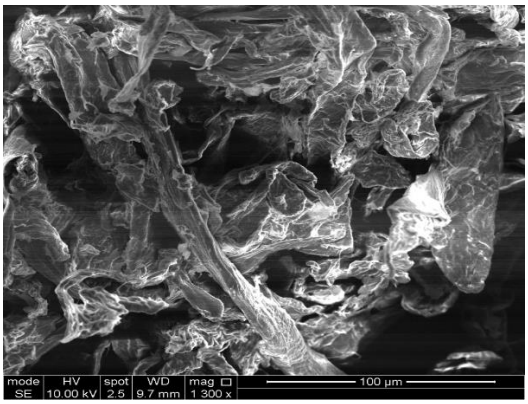

Figure 6: SEM micrograph showing the morphology (c) CNC Acetate (OPF)

Fig. 6 shows the SEM morphology of the (a) cellulose having a long twisted cluster of coiled particles, while (b) CNF is a whorl of broken cluster of the coiled fibril. This result shows a little increment in the crystalline region and a reduction in the amorphous region.

Table 3: Change in Bioplastic's Mass Before and after degradation

Bioplastic	Initial mass	Final mass	Percentage Loss (%)
Sample A (0ml glycerol)	0.29	0.05	82.76
Sample B (1ml glycerol)	0.31	0.047	84.83
Sample C (2ml glycerol)	0.34	0.03	91.18

The observed results of the three mass of bioplastics before and after degradation are shown on Table 3. Bioplastic was reduced by an average mass of 86.26% after being buried in the soil-compost mixture for 28 days. This proved that bioplastics are easier to degrade than conventional plastics which were non-biodegradable. This bioplastic was easily degraded due to the amorphous form of a polymer so that microorganisms in the soil could attack the bioplastic molecules. The pattern of degradation observed indicates the more the glycerol added the greater the degradation as more amorphous regions will be created in the sample.

Table 4: Mechanical Testing (Hardness) for Synthesized Bioplastic

Bioplastic	Average Brinell Hardness (HB)
Sample A (0ml glycerol)	11.97
Sample B (1ml glycerol)	11.37
Sample C (2ml glycerol)	9.97

Table 4: The bioplastic synthesized showed a progressive hardness property as the amount of glycerol used reduces. Sample A (without glycerol) has an hardness of 11.97 kgf/mm^2, while Sample B (with 1 ml glycerol) had a reduced hardness of 11.37 kgf/mm^2 and Sample C (with 2 ml glycerol) further reduced in hardness 9.97 kgf/mm^2. This can be attributed to the crystalline cellulose in the samples. The force of contact during the bonding of the polymeric substance decreases with increasing glycerol concentration. Glycerol may also improve bioplastics' flexibility and molecular mobility, making them more elastic and breaking-elongation-enhancing as postulated by Rohmawati *et al.*, 2018.

Table 5: (a) Crystalline size and Crystallinity index of the synthesized bioplastic

Bioplastic	Angle (2θ)	FWHM (degree)	Crystalline size (nm)	Crystallinity index
Sample A(0ml glycerol)	22.5	2.4	4.08	88.5
Sample B (1ml glycerol)	22.4	1.54	5.83	82.6
Sample C (2ml glycerol)	22.5	1.32	6.23	79.8

Table 5 shows the crystalline size and crystallinity index of the bioplastic synthesized indicates Sample A is 88.5%, Sample B is 82.6%, Sample C is 79.8%. The effect of crystallinity index indicates the amount of crystal present in the sample. Most crystalline matter improves strength of the material. The result also shows the particles are within nano scale (from 4.08nm to 6.23nm).

TABLE 6: TENSILE STRENGTH AND ELONGATION

Sample	Glycerol Vol. used (ml)	Tensile strength (MPa)	Elongation (%)
A	0	6.08	2.75
B	1	8.00	3.5
C	2	52.00	3.75

The best attribute for plastic films is to maximize the tensile strength. This is because a greater tensile strength value means the film can survive damage from mechanical interference (Ornelas *et al*., 2023). There was considerable increase in this property as the amount of glycerol was increased showing a remarkable strength of 6.08 MPa as the minimum exceed the minimum value of 1.343 MPa according to the Biodegradable plastic standard by SNI 7818:2014 (Gabriel *et al.*, 2021). The increase in the tensile strength of this bioplastic can be attributed to the increase in crystallinity of the cellulose nanocrystal which was observed by Gabriel *et al.*, 2021 as it relates to amylose and amylopectin content of starch in producing bioplastics. It observed that compared to amylopectin, which is amorphous, high amylose tends to form crystals with more considerable mechanical characteristics.

Between cellulose and glycerol, there existed a hydrogen bond interaction. Furthermore, adding glycerol may make bioplastics more flexible and enhance molecular mobility, making them more elastic and capable of higher breaking elongation (Rohmawati *et al*., 2018). The increase in elongation was not as exponential as observed from 2.75% (0 ml glycerol) to 3.5% (1 ml glycerol) and to 3.75% (2 ml glycerol).

FTIR Results

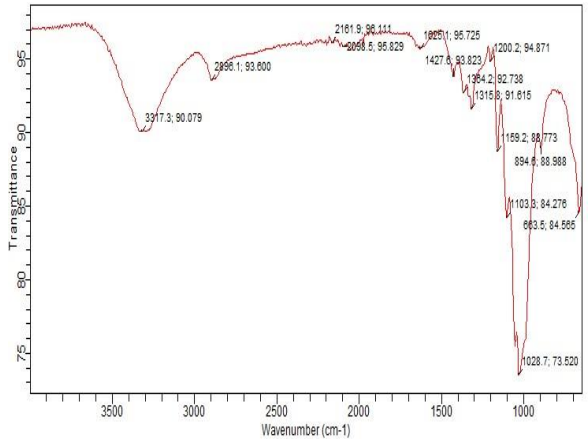

Figure 8: FT-IR spectra (a) cellulose from OPF

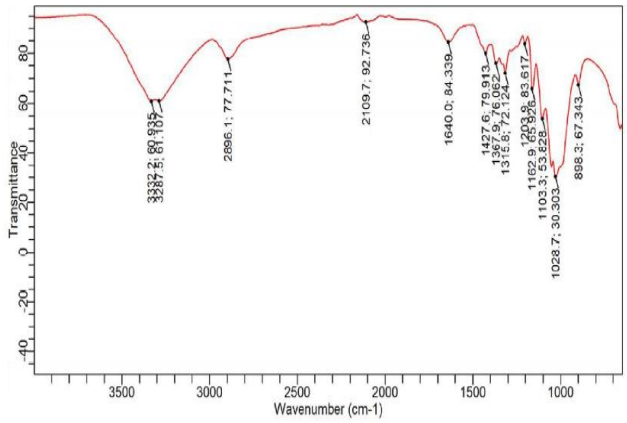

Figure 8: FT-IR spectra (b) CNC OPF

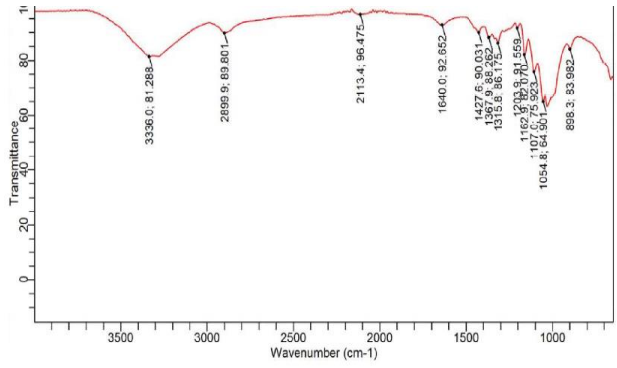

Figure 8: FT-IR spectra (c) CNC acetate from OPF

Figure 8 shows the spectra from FT-IR (a) cellulose indicates peaks at 3317.3 cm^{-1} a weak broad OH- stretching vibration, 2896.1 cm^{-1} C-H stretching vibrate of the alkane family and O- bending vibration in the fingerprint regions characteristic peaks at 1364.2 cm^{-1}, 1315.8 cm^{-1} and 1028.7 cm^{-1}. (b) CNC indicates two prominent peaks at 3332.2 cm^{-1} and 3287.5 cm^{-1} weak, broad OH- stretching vibration, 2896.1 cm^{-1} C-H stretching vibrate of the alkane family, a monosubstituted weak stretching vibration of C≡C at 2109.7 cm^{-1}. Another notable peak is that of a carbonyl

(C=O) peak at 1640.0 cm^{-1}. This could be attributed to the acid hydrolysis on the cellulose to reduce the amorphous region on the cellulose. (c) CNC acetate indicates peaks at 3336.0 cm^{-1} a weak, broad OH- stretching vibration, 2899.9 cm^{-1} C-H stretching vibrate of the alkane family and carbonyl (C=O) peak at 1640.0 cm^{-1} subjective of the acetylation process.

Cellulose Acetate degree of Substitution

According to Rohmawati *et al.*, 2018, the polysaccharide's average rate of substitution for each unit of glucose is represented by the degree of substitution (DS) value. The DS value is 3 if all of the hydroxyl groups in each unit of glucose are esterified. The cellulose ester's plastic characteristics increase with increasing DS value. Free hydroxyl groups at the C2, C3, and C6 atoms in cellulose may be changed to acetyl groups during acetylation. The greatest DS value is thus, in principle, 3. The addition-elimination process causes substitution to happen.

The reactivity of three free hydroxyl (-OH) groups varies. Due to steric restrictions, the -OH group in C6 atoms is more reactive and acetylates more quickly than -OH groups in C2 and C3 atoms. The -OH group at C2 is more reactive compared to the -OH groups at C3 atoms. This is possibly due to the -OH group at C2 is more acidic and closer to hemiacetal than the -OH group at C3 atoms (Rohmawati *et al.*, 2018). The value for the synthesized cellulose acetate was 1.6.

Conclusion and Recommendation

Conclusion

Agricultural biomass can be a useful material and a sustainable one for the synthesis of bioplastic. The yield of cellulose from Oil palm pressed fibre (38.45 %) shows that this agro-waste can be optimized. Acid hydrolysis, which is the process used in achieving more crystalline regions in the extracted cellulose, can be processed using a recyclable organic acid (maleic acid) rather than the conventional inorganic acid. Acetylation of the cellulose nanocrystal (CNC) enables the polymerization process. The crystallinity index of the bioplastic shows some interesting result which is evident in the mechanical test conducted to suggest a better strength could be achieved also.

Recommendation

With the intense work on reducing conventional plastic menace on man and its environment, nano-sized bioplastic could provide a viable as well as solve some problems associated with the agricultural waste disposal.

References

De-france, K., Hoare, T., and Cranston, E. (2017). "Nanocellulose Review". Chemistry of material 29(11): 4609-4631.

Feng, J., and You, L. (2015) Cellulose Nano crystal isolation from tomato peels and assembled Nano fibers. *Fiber and polymer science*.

Fortunati, E., Peltzer, M., Armentano, I., Torre, L., Jimenez, A., & Kenny, J. M. (2012). Effects of modified cellulose nanocrystals on the barrier and migration properties of PLA nano-biocomposites. *Carbohydrate Polymers*, **90**, 948-956.

Gabriel, Azmi & Solikhah, Anggita & Rahmawati, Alifia. (2021). Tensile Strength and Elongation Testing for Starch-Based Bioplastics using Melt Intercalation Method: A Review. *Journal of Physics*: Conference Series: 1, 1742-6596.

Huan, M. F., Yu, J. G., & Ma, X. F. (2006) High mechanical performance MMT-urea and formamide-plasticized thermoplastic cornstarch biodegradable nanocomposites. *Carbohydrate Polymers*, **63**, 393–399.

Jiang, Z., Ngai, T. (2022). Recent Advances in Chemically Modified Cellulose and Its Derivatives for Food Packaging Applications: A Review. *Polymers*, **14**: 15-33.

Kassab Z., Abdellaoui Y., Salim M. H., Bouhfid R., Qaiss A. E., El Achaby M. (2020). "Micro- and nano-celluloses derived from hemp stalks and their effect as polymer reinforcing materials", *Carbohydrate Polymers*, 245, 11 – 26.

Kibar, E. and Us, F. (2013). Thermal, mechanical and water adsorption properties of corn starch-carboxymethyl cellulose/methylcellulose biodegradable films. *Journal of Food Engineering*, 114, 123-131.

Klemm, D., Cranston, E., Fischer, D., Gama, M., Kedzior, S., Kralisch, D., Kramer, F., Kondo, T., Lindstrom, T., and Nietzsche, S. (2018). Nanocellulose as a natural source for groundbreaking applications in materials science: today's state. Mater Today 21:720–748.

Kristina, J., Ulf, G., Djem, K., Thomas, H., and Helena L. (2004). Effect of pulp composition on the characteristics of residuals in CMC made from each pulps. *Cellulose* **12**: 383-393

Kumar, R., Sharma, R., and Singh, A. (2017). Cellulose based biosorbents; journey from lignocellulose biomass to toxic metal ions sorption application- a review. J.mol.Liq. **232**, 62-93.

Lam E, Male KB, Chong JH, Leung ACW, Luong JHT. (2012). Applications of functionalized and nanoparticle-modified nanocrystalline cellulose. Trends Biotechnol; **30**: 283–90.

Lawal O.S., Adebowale K.O., Ogunsanwo B.M., Barba L.L., Ilo N.S. (2005). Oxidized and acid thinned starch derivatives of hybrid maize: functional characteristics, wide-angle X-ray diffractometry and thermal properties, *International Journal of Biological Macromolecules*, **35**: (2), 71-79.

Lee, K.-Y., Quero, F., Blaker, J. J., Hill, C. A. S., Eichhorn, S. J., & Bismarck, A. (2011). Surface only modification of bacterial cellulose nanofibres with organic acids. *Cellulose*, **18**, 595-605.

Morandi, G., Heath, L., & Thielemans, W. (2009). Cellulose nanocrystals grafted with polystyrene chains through surface-initiated atom transfer radical polymerization (SI-ATRP). *Langmuir*, **25**, 8280-8286.

Morgan, E. (2018) "Cellulose physical properties". eye glass frame materials,**12**(3): 476-578.

Rhim, J. W., Park, H. M., & Ha, C. S. (2013). Bio-nanocomposites for food packaging applications. *Progress in Polymer Science*, **38**, 1629 – 1650.

Rohmawati B., Sya'idah F. A., Rhismayanti, Alighiri D. and Eden W. T. (2018). Synthesis of Bioplastic-based Renewable Cellulose Acetate from Teak Wood (Tectona grandis) Biowaste Using Glycerol-Chitosan Plasticizer, *Oriental Journal of Chemistry*, **34**:4, 1810 – 1816.

Seta F. T., An X., L. L., Zhang H., Yang J., Zhang W., Nie S., Yao S., Cao H., Xu Q., Bu Y., Liu H. (2020). Preparation and characterization of high yield cellulose nanocrystals (CNC) derived from ball mill pretreatment and maleic acid hydrolysis, *Carbohydrate Polymers*, **234:** 1 – 10.